Supplementary Information (SI) for Journal of Materials Chemistry A.

Surface Modification of Copper Oxide Nanosheets with CeO_2 for Enhanced CO_2 reduction to C_2H_4

Shuaibing Yang[a], Fanfei Sun[c], Rong Cao[a][b], and Minna Cao[a][b]*

[a] State Key Laboratory of Structural Chemistry, Fujian Institute of Research on the Structure of Matter, Chinese Academy of Sciences, Fuzhou 350002, P.R. China

[b] University of Chinese Academy of Sciences, Beijing 100049, P.R. China

[c] Shanghai Synchrotron Radiation Facility, Shanghai Institute of Applied Physics, Chinese Academy of Sciences, Shanghai 201204, P. R. China

Corresponding Author: mncao@fjirsm.ac.cn (M. Cao)

Materials characterizations

Inductively coupled plasma optical emission spectroscopy (ICP-OES) measurements were tested on an Ultima 2 analyzer (Jobin Yvon). Transmission electron microscopy (TEM) images, high-resolution TEM (HRTEM) images, and corresponding energy-dispersive X-ray spectroscopy (EDS) elemental mapping images were recorded by Titan Cubed Themis G2 300 (FEI) high-resolution transmission electron microscope operated at 200 kV. X-ray diffraction (XRD) tests were performed on a Miniflex 600 diffractometer using Cu Kα radiation (λ = 0.154 nm). X-ray photoelectron spectroscopy (XPS) were conducted by an ESCALAB 250Xi X-ray photoelectron spectrometer (Thermo Fisher) using an Al Kα source (15 kV, 10 mA). For reaction selectivity analysis, the gas products were detected by the FULI INSTRUMENTS GC9790Plus gas chromatograph (GC) equipped with FID and TCD, and liquid products were tested by ^{1}H NMR on Bruker AVANCE AV III 600. The electrochemical performance measurements were conducted on a CHI1140C electrochemical workstation. The XAFS were collected at the beamline BL14W1 station of the Shanghai Synchrotron Radiation Facility (SSRF), China. The Raman experiments were performed on the Labram HR800 Evolution Raman spectrometer (HORIBA Jobin Yvon). *In situ* attenuated total reflection Fourier-transform infrared spectra (ATR-FTIR) were conducted on a Thermo Scientific Nicolet iS50.

Supplementary Figures and tables

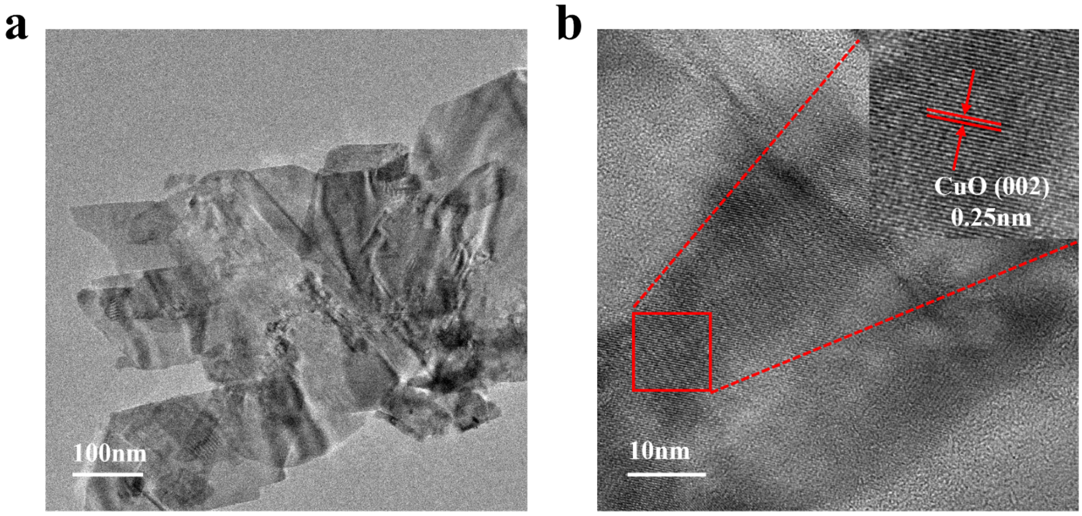

Fig. S1 (a) TEM image, and (b) HR-TEM image of CuO NSs.

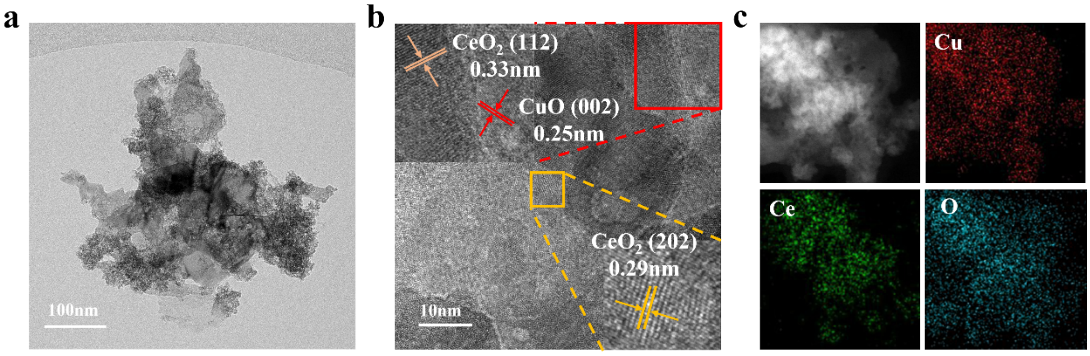

Fig. S2 (a) TEM, (b) HR-TEM, and (c) EDS mapping of CeO_2/CuO NSs-1.

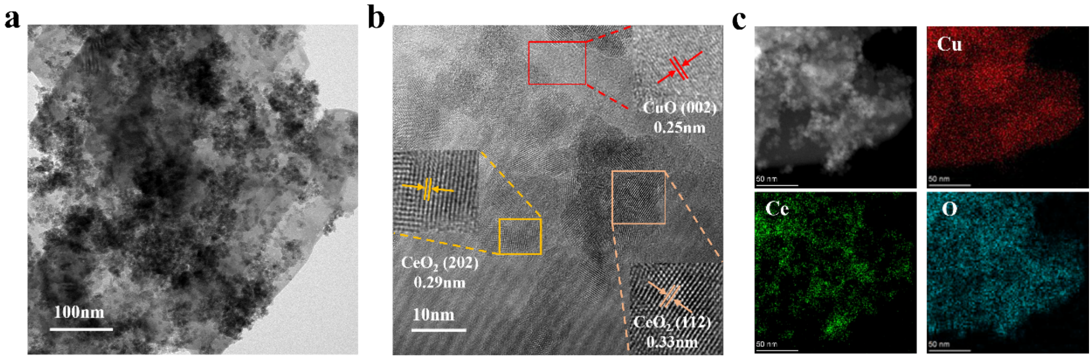

Fig. S3 (a) TEM, (b) HR-TEM, and (c) EDS mapping of CeO_2/CuO NSs-3.

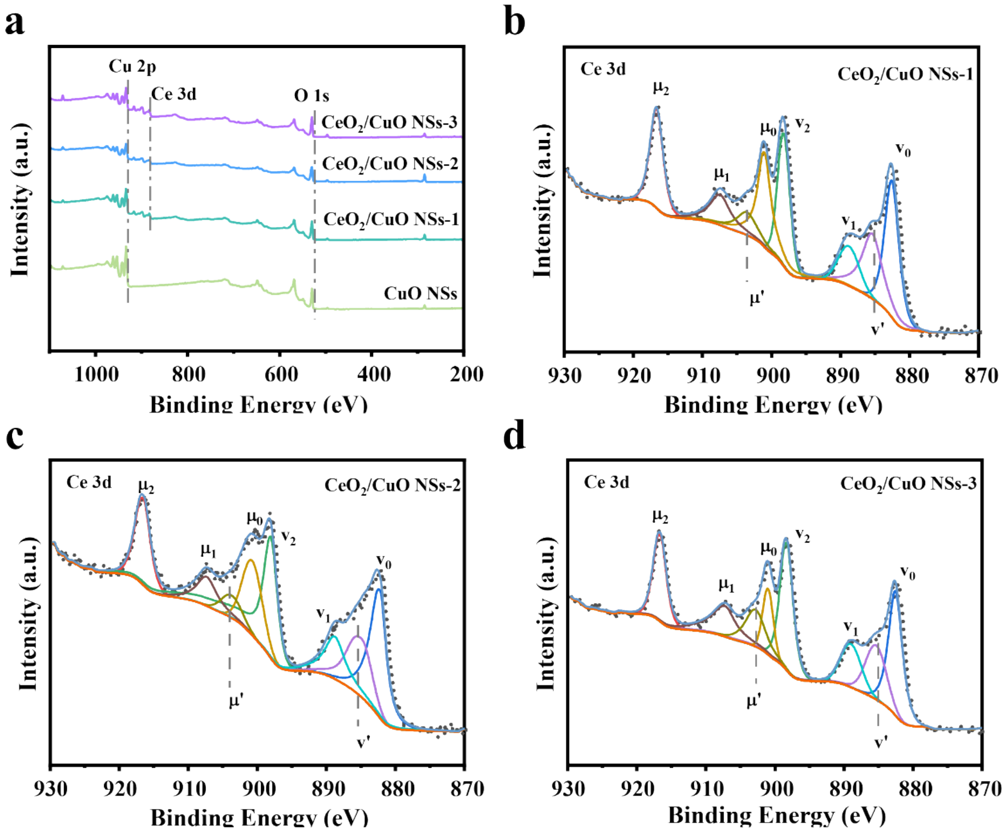

Fig. S4 (a) The overall survey spectra of the CuO NSs and CeO_2 modified CuO catalysts. High-resolution Ce 3d XPS spectra of (b) CeO_2/CuO NSs-1, (c) CeO_2/CuO NSs-2, and (d) CeO_2/CuO NSs-3.

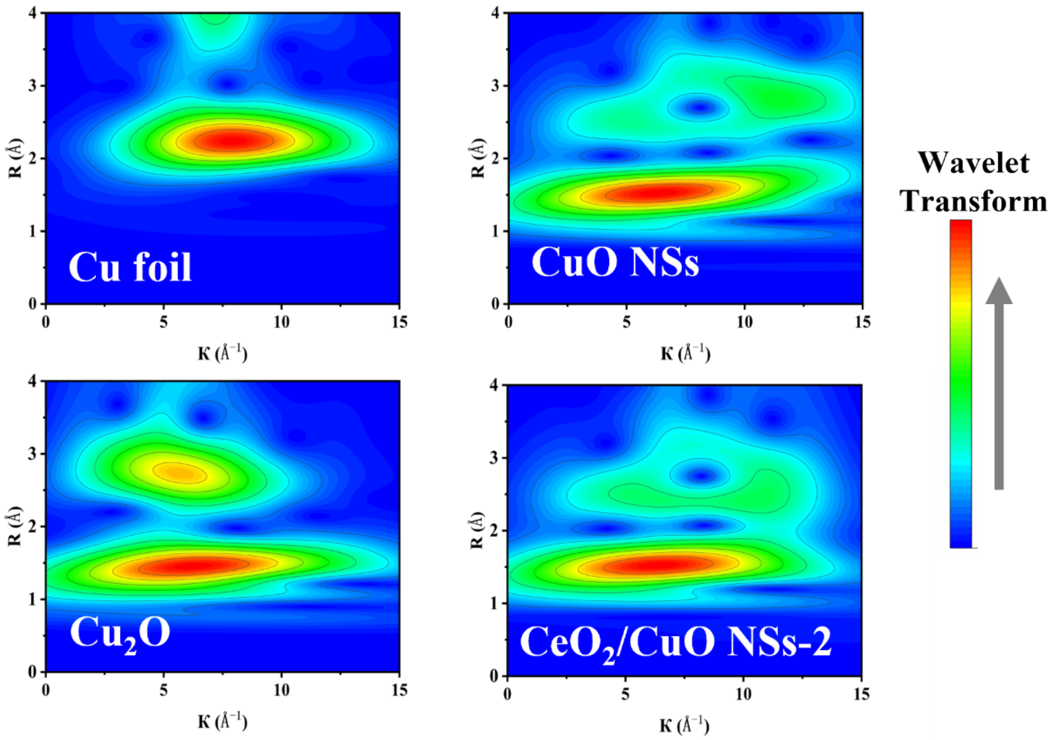

Fig. S5 Wavelet transformed k3-weighted EXAFS of CeO_2/CuO NSs-2, CuO NSs, Cu_2O, and Cu foil.

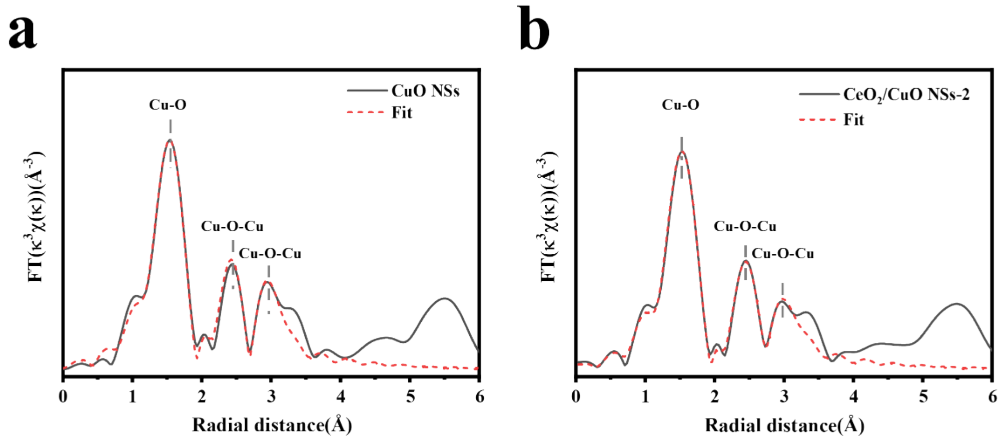

Fig. S6 Experimental and fitting K-edge EXAFS spectra for (a) CuO NSs and (b) CeO_2/CuO NSs-2

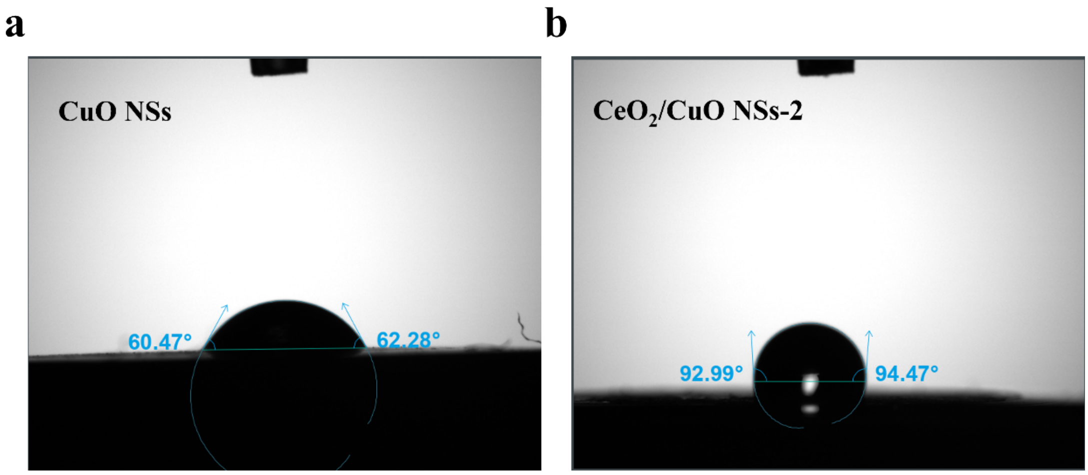

Fig. S7 Water contact angle measurement images of (a) CuO NSs, and (b) CeO_2/CuO NSs-2.

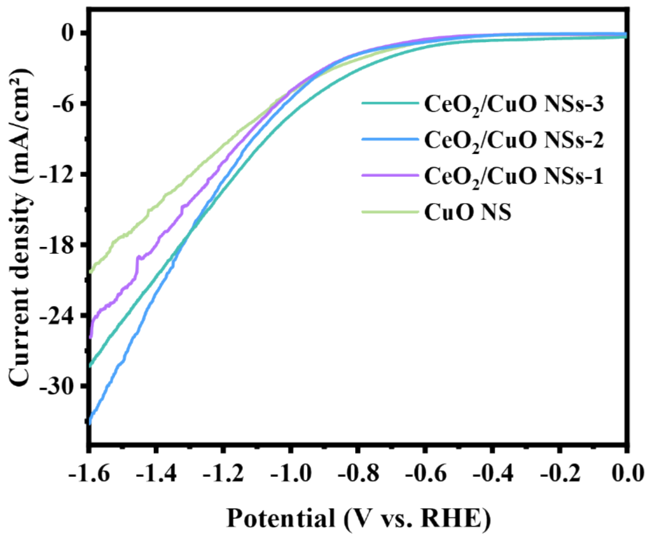

Fig. S8 LSV curves for difference samples in CO_2 saturated electrolyte in a H-Cell with 0.1M $KHCO_3$ + 0.1M KCl.

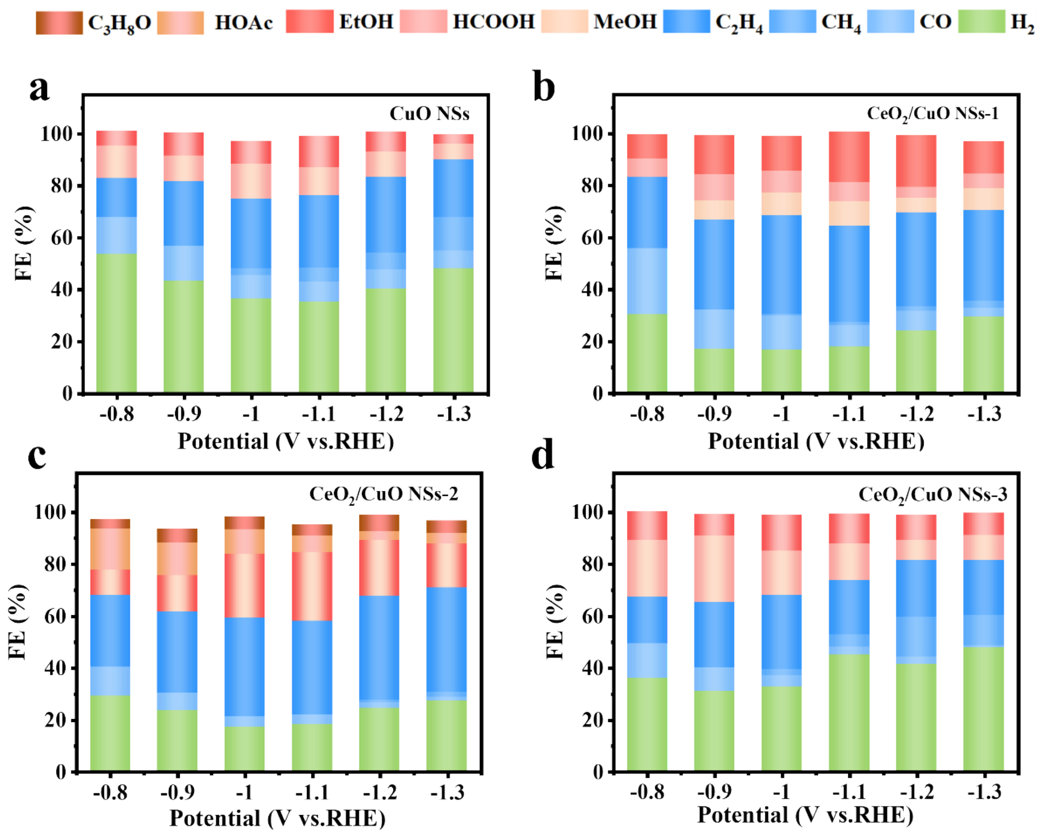

Fig. S9 The selectivity of CO_2RR in H-Cell with 0.1M $KHCO_3$ + 0.1M KCl for (a) CuO NSs, (b) CeO_2/CuO NSs-1, (c) CeO_2/CuO NSs-2, and (d) CeO_2/CuO NSs-3 at different potentials.

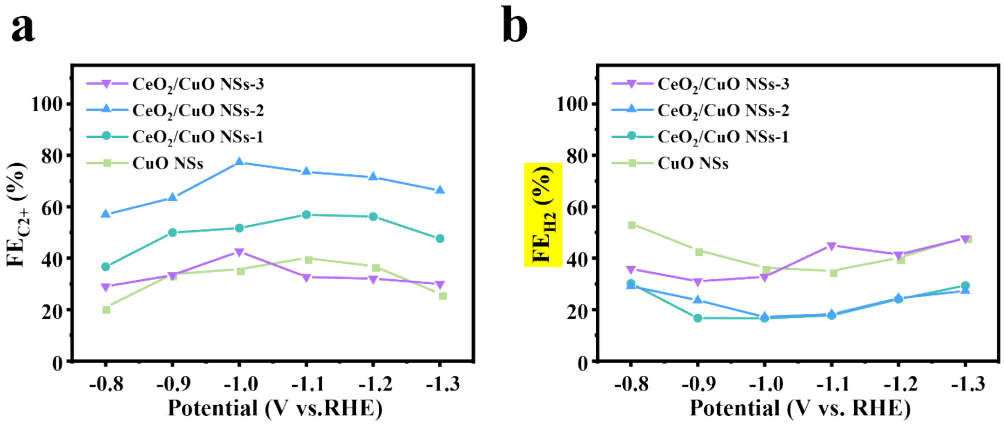

Fig. S10 (a) Faradaic efficiencies of C_{2+} over different samples at different potential in a H-Cell. (b) Faradaic efficiencies of H_2 over different samples at different potential in a H-Cell with 0.1M $KHCO_3$ + 0.1M KCl.

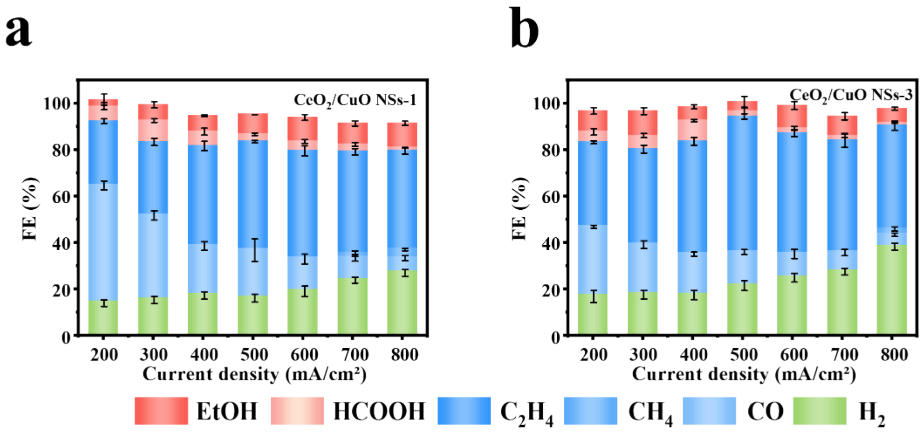

Fig. S11 The selectivity of CO_2RR in Flow Cell with 1M KOH for (a) CeO_2/CuO NSs-1, and (b) CeO_2/CuO NSs-3 at different potentials.

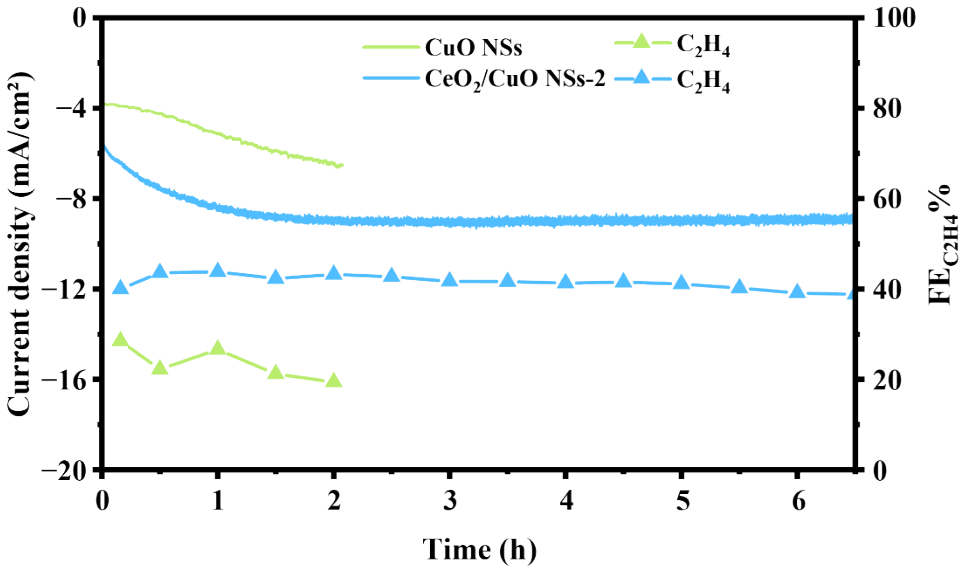

Fig. S12 Stability test of CeO_2/CuO NSs-2 and CuO NSs at -1.0V vs. RHE in H-Cell.

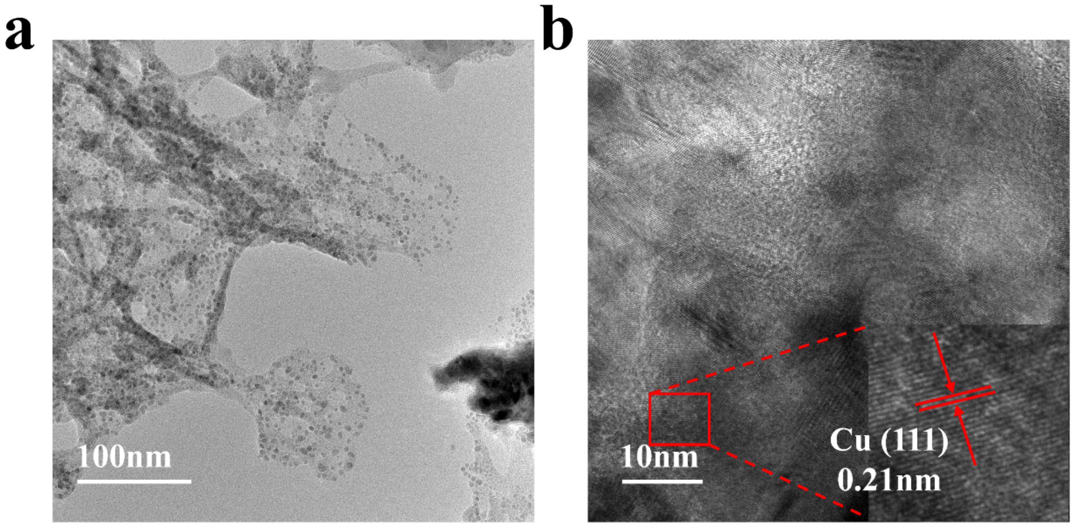

Fig. S13 (a) TEM, and (b) HR-TEM of CuO NSs after 0.5h CO_2RR at -1.0V vs. RHE.

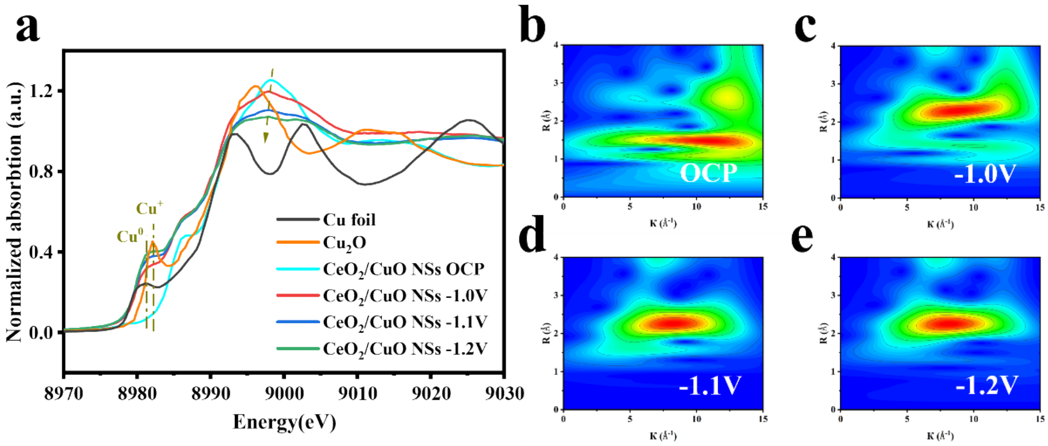

Fig. S14 (a) Cu K-edge XANES spectra, (b) Wavelet transformed k3-weighted EXAFS of CeO_2/CuO NSs-2 at different potential.

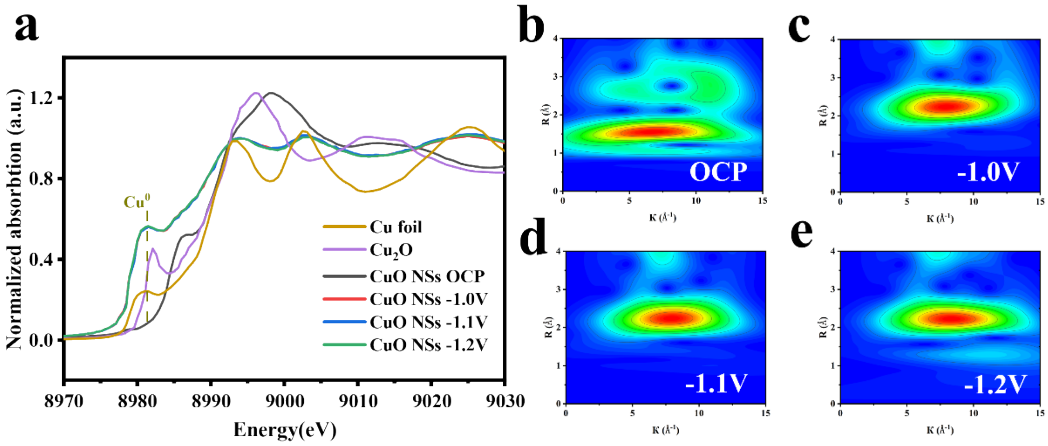

Fig. S15 (a) Cu K-edge XANES spectra, (b) Wavelet transformed k3-weighted EXAFS of Cu_7CeO_x NSs at different potential.

Table S1 Ratio of elements determined by ICP-OES

Samples	Weight fraction (%)		Cu : Ce
	Cu	Ce	
CeO_2/CuO NSs-1	64.16	14.25	9.92 : 1
CeO_2/CuO NSs-2	46.18	12.13	8.39 : 1
CeO_2/CuO NSs-3	53.44	18.02	6.52 : 1

Table S2 Ratio of elements determined by XPS

Samples	Cu (%)	Ce (%)
CuO NSs	100	
CeO_2/CuO NSs-1	68.75	31.25
CeO_2/CuO NSs-2	62.96	37.04
CeO_2/CuO NSs-3	58.33	41.67

Table S3 Comparison of the C_2H_4 selectivity of the present work with that of the catalysts reported in the literature.

Catalyst	Current density (mA/cm²)	FE%	Electrolyte	Ref.
CeO_2/CuO NSs-2	600	64.1 %	1 M KOH	This work
Cu/Ni-NAC	100	66%	10 M KOH	Ref. 1
MgAl-LDH/Cu	300	55.1%	1 M $KHCO_3$	Ref. 2
$La(OH)_3$/Cu	1000	40.8%	1 M KOH	Ref. 3
CuAg film	300	60%	1 M KOH	Ref. 4
Cu nanowires with surface steps	23	77%	0.1 M $KHCO_3$	Ref. 5
p-CuO_x-Cu	14	42%	0.1 M $KHCO_3$	Ref. 6

References

1. Z. Yin, J. Yu, Z. Xie, S.-W. Yu, L. Zhang, T. Akauola, J. G. Chen, W. Huang, L. Qi and S. Zhang, *J. Am. Chem. Soc*., 2022, **144**, 20931-20938.
2. Y. N. Xu, W. Li, H. Q. Fu, X. Y. Zhang, J. Y. Zhao, X. Wu, H. Y. Yuan, M. Zhu, S. Dai, P. F. Liu and H. G. Yang, *Angew. Chem. Int. Ed*., 2023, **62**, e202217296.
3. S. Hu, Y. Chen, Z. Zhang, S. Li, H. Liu, X. Kang, J. Liu, S. Ge, J. Wang, W. Lv, Z. Zeng, X. Zou, Q. Yu and B. Liu, *Small*, 2024, **20**, 2308226.
4. T. T. H. Hoang, S. Verma, S. Ma, T. T. Fister, J. Timoshenko, A. I. Frenkel, P. J. A. Kenis and A. A. Gewirth, *J. Am. Chem. Soc.*, 2018, **140**, 5791-5797.
5. C. Choi, S. Kwon, T. Cheng, M. Xu, P. Tieu, C. Lee, J. Cai, H. M. Lee, X. Pan, X. Duan, W. A. Goddard and Y. Huang, *Nat. Catal.*, 2020, **3**, 804-812.
6. J. Fu, H. Zhang, H. Du, X. Liu, Z.-H. Lyu, Z. Jiang, F. Chen, L. Ding, T. Tang, W. Zhu, D. Su, C. Ling, J. Wang and J.-S. Hu, *J. Am. Chem. Soc.*, 2024, **146**, 23625-23632.